Vanishing Parotid Tumors on MR Imaging

Eiji Matsusue,* Yoshio Fujihara,* Eiken Matsuda,† Yusuke Tokuyasu,‡ Shu Nakamoto,‡ Kazuhiko Nakamura* and Toshihide Ogawa§

**Department of Radiology, Tottori Prefectural Central Hospital, Tottori 680-0901, Japan, †Department of Otorhinolaryngology, Tottori Prefectural Central Hospital, Tottori 680-0901, Japan, ‡Department of Pathology, Tottori Prefectural Central Hospital, Tottori 680-0901, Japan, and §Division of Radiology, Department of Pathophysiological and Therapeutic Science, School of Medicine, Tottori University Faculty of Medicine, Yonago 683-8503, Japan*

ABSTRACT

Background Of all parotid gland tumors, only oncocytoma has been reported to appear isointense to the parotid gland, namely vanishing, on fat-saturated T2 and T1 postcontrast gadolinium-enhanced magnetic resonance imaging (MRI). The purpose of this study was to evaluate vanishing of parotid tumors on conventional MRI with and/or without postcontrast gadolinium-enhancement and on diffusion weighted imaging (DWI).

Methods In 8 of 51 patients, ten parotid gland tumors had homogeneously enhanced lesions and were retrospectively analysed. Comparisons of signal intensity between those parotid tumors and parotid glands and evaluations of vanishing were performed on T1-weighted imaging (T1WI), T2-weighted imaging (T2WI), fat-suppressed T2WI (FS-T2WI), postcontrast gadolinium-enhanced T1WI (CE-T1WI) and fat-suppressed CE-T1WI (FS-CE-T1WI), DWI as well as apparent diffusion coefficient (ADC).

Results Ten parotid gland tumors consisted of five Warthin tumors, two pleomorphic adenomas, two parotid carcinomas (small cell carcinoma and adenoid cystic carcinoma) and one oncocytoma. All tumors showed hypointensity on T1WI and hyperintensity on DWI. Nine of ten tumors showed vanishing on the other MR sequences. All Warthin tumors showed vanishing on FS-T2WI, FS-CE-T1WI and the ADC map. One oncocytoma showed vanishing on FS-T2WI and the ADC map and hyperintensity on FS-CE-T1WI. All pleomorphic adenomas showed vanishing on T2WI and CE-T1WI. One adenoid cystic carcinoma showed vanishing only on CE-T1WI.

Conclusion Vanishing of parotid tumors can be observed not only on FS-T2WI and FS-CE-T1WI but also on T2WI, CE-T1WI and ADC mapping.

Key words magnetic resonance imaging; oncocytoma; parotid tumor; vanishing; Warthin tumor

Computed tomography (CT), magnetic resonance imaging (MRI) and ultrasonography are commonly used to evaluate parotid gland lesions. Several parotid gland lesions, such as pleomorphic adenoma, are occasionally invisible on contrast-enhanced CT; the conspicuity of these lesions can be reduced due to a combination of the high density of the parotid gland and weak enhancement of the lesion.[1] Meanwhile, of all parotid gland tumors, only oncocytoma has been reported to appear isointense to the parotid gland, namely vanishing on fat-saturated T2 and T1 postcontrast gadolinium-enhanced MRI.[2] However, there have been no reports evaluating whether any other parotid tumors show vanishing on various MR sequences. The vanishing of parotid tumors on MRI requires tumor homogeneity and isointensity to the normal parotid gland. Furthermore, the contrast of signal intensity between parotid tumors and normal parotid glands can be altered due to the extent of tumor contrast enhancement on postcontrast gadolinium-enhanced MRI and due to the extent of fat suppression of parotid glands with physiological fat deposition on fat-suppressed MRI. Generally, large tumors can be inhomogeneous due to necrosis, degeneration or hemorrhage. Therefore, tumor vanishing is considered to be a feature of small tumors on MRI. The purpose of this study was to evaluate vanishing of parotid tumors on conventional MRI with and/or without postcontrast gadolinium-enhancement and on diffusion weighted imaging (DWI).

MATERIALS AND METHODS

Patients

Between April 2010 and May 2016, MRI examinations were performed on 51 consecutive patients suspected of parotid tumors in our hospital. Of the 51 patients, thirty-nine patients underwent gadolinium-enhanced MRI and DWI. Of the 39 patients, only eight patients who had

Corresponding author: Eiji Matsusue, MD, PhD
matsusuee@tp-ch.jp
Received 2017 November 29
Accepted 2017 December 21
Abbreviations: ADC, apparent diffusion coefficient; CE-T1WI, postcontrast gadolinium-enhanced T1-weighted imaging; CT, computed tomography; DWI, diffusion-weighted imaging; FS-CE-T1WI, fat-suppressed CE-T1WI; FS-T2WI, fat-suppressed T2-weighted imaging; MRI, magnetic resonance imaging; T1WI, T1-weighted imaging; T2WI, T2-weighted imaging

Table 1. MRI features of parotid tumors

Patient No.	Age (years) /Sex	Diagnosis	Volume (cm^3)	Size (cm)	T1WI	T2WI	CET1WI	FST2WI	FSCET1WI	DWI	ADC	ADC value ($\times 10^{-3}$ mm^2/s)
1	61/M	Warthin tumor	0.9	1.2	Low	Low	Low	Iso	Iso	High	Iso	0.84
2	52/M	Warthin tumor	5.4	2.2	Low	Low	Low	Iso	Iso	High	Iso	0.88
3	56/M	Warthin tumor	2.5	1.7	Low	Low	Low	Iso	Iso	High	Iso	0.96
3	56/M	Warthin tumor	10.7	2.8	Low	Low	Low	Iso	Iso	High	Iso	1.13
3	56/M	Warthin tumor	7.6	2.5	Low	Low	Low	Iso	Iso	High	Iso	1.05
4	75/F	Oncocytoma	0.9	1.2	Low	Low	Low	Iso	High	High	Iso	1.09
5	53/F	Pleomorphic adenoma	0.2	0.7	Low	Iso	Iso	High	High	High	High	1.51
6	42/M	Pleomorphic adenoma	1.1	1.3	Low	Iso	Iso	High	High	High	High	1.41
7	59/M	Small cell carcinoma	4.1	2	Low	Low	Low	High	High	High	Low	0.73
8	61/F	Adenoid cystic carcinoma	0.3	0.9	Low	Low	Iso	High	High	High	High	1.29

ADC, apparent diffusion coefficient; CE-T1WI, postcontrast gadolinium-enhanced T1-weighted imaging; DWI, diffusion-weighted imaging; F, female; FS-CE-T1WI, fat-suppressed CE-T1WI; FS-T2WI, fat-suppressed T2-weighted imaging; M, male; MRI, magnetic resonance imaging; T1WI, T1-weighted imaging; T2WI, T2-weighted imaging.

homogeneously enhanced lesions (3 females, 5 males; median age, 56 years; range, 42–75 years; number of lesions, 10 parotid gland tumors) were included in the present study and retrospectively analysed. Histopathological diagnoses were made on the basis of findings in specimens obtained at surgical resection (Table 1). This retrospective study was approved by the institutional review board of our institution, and the informed consent requirement was waived.

MRI

MR examinations were performed within two months before surgery in all patients. MRI was performed using a 1.5T MRI system (Excite HD; GE Healthcare, Milwaukee, WI) with head and neck array coils. The parameters for T1 and T2 weighted imaging (T1WI, T2WI) were as follows. For the axial pre and postcontrast gadolinium-enhanced T1-weighted spin-echo sequence, the parameters were repetition time, 500 msec; echo time, 8 msec; matrix, 256 × 256; section thickness, 5 mm; intersection gap, 1 mm; field of view, 22 cm; and two signals averaged. For the axial T2-weighted fast spin-echo sequence, the parameters were repetition time, 3500 msec; echo time, 90msec; matrix, 256 × 256; section thickness, 5 mm; intersection gap, 1mm; field of view, 22 cm; and two signals averaged. For the axial fat-suppressed T2-weighted fast spin-echo sequence, the parameters were repetition time, 4300 msec; echo time, 90 msec; matrix, 256 × 256; section thickness, 5 mm; intersection gap, 1mm; field of view, 22 cm; and two signals averaged. For the postcontrast gadolinium-enhanced 3D fat-suppressed T1-weighted multiphase spoiled gradient recalled sequence, the parameters were repetition time, 5msec; echo time, 2.5 msec; matrix, 256 × 256; effective section thickness, 2 mm; field of view, 22 cm; and three signals averaged. The parameters for diffusion-weighted imaging were as follows for the axial spin-echo single-shot echo-planar sequence: repetition time, 4300 msec; echo time, 80msec; matrix, 128 × 128; section thickness, 5-mm, intersection gap, 1-mm; field of view, 22 cm; and two signals averaged. Sensitizing diffusion gradients were applied sequentially in the x, y, and z directions with b values of 0 and 800 sec/mm^2. Apparent diffusion coefficient (ADC) maps were also generated.

Evaluations of MR images

One author (E.M., 20 years of experience in head and neck MR imaging) evaluated the MR images obtained by T1WI, T2WI, fat-suppressed T2WI (FS-T2WI), postcontrast gadolinium-enhanced T1WI (CE-T1WI) and fat-suppressed CE-T1WI (FS-CE-T1WI), DWI and ADC mapping. The approximate tumor volume was calculated from the product of tumor length, width, and depth and the multiplication factor $\pi/6$. The signal intensity (SI) in each sequence was visually judged as 'low' (hypointensity) when the SI of the tumor was lower than that of the parotid tissue, 'iso' (isointensity) when the SI was equal to that of the parotid tissue, and 'high' (hyperintensity) when the SI was brighter than that of the parotid tissue.

RESULTS

Table 1 shows the MRI features of the ten parotid gland tumors, which comprised five Warthin tumors, one oncocytoma, two pleomorphic adenomas and two parotid carcinomas (small cell carcinoma and adenoid cystic carcinoma) in eight patients. One patient had three Warthin tumors. The average volume of all tumors was

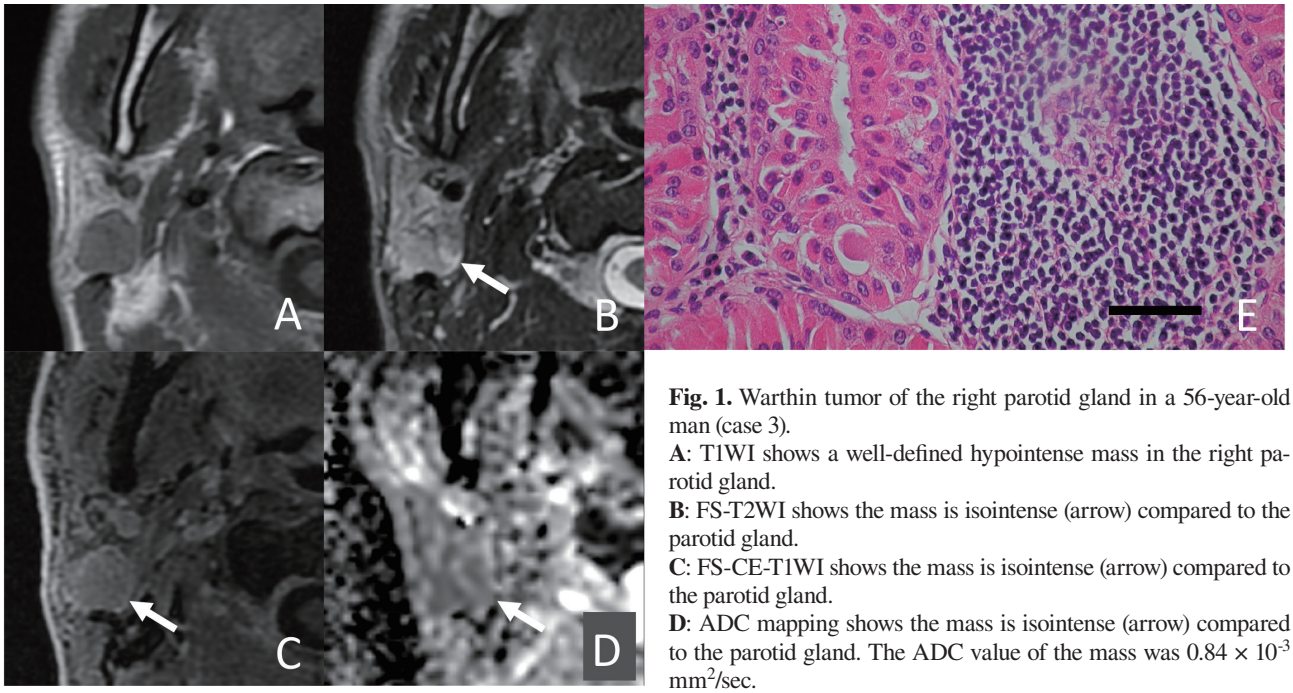

Fig. 1. Warthin tumor of the right parotid gland in a 56-year-old man (case 3).
A: T1WI shows a well-defined hypointense mass in the right parotid gland.
B: FS-T2WI shows the mass is isointense (arrow) compared to the parotid gland.
C: FS-CE-T1WI shows the mass is isointense (arrow) compared to the parotid gland.
D: ADC mapping shows the mass is isointense (arrow) compared to the parotid gland. The ADC value of the mass was 0.84×10^{-3} mm^2/sec.
E: High-power view showing proliferation of the glandular epithelium with oncocytic cytoplasm (left) and lymphoid stroma (right) (hematoxylin-eosin, scale bar = 25 μm).
ADC, apparent diffusion coefficient; FS-CE-T1WI, fat-suppressed postcontrast gadolinium-enhanced T1-weighted imaging; FS-T2WI, fat-suppressed T2-weighted imaging; T1WI, T1-weighted imaging.

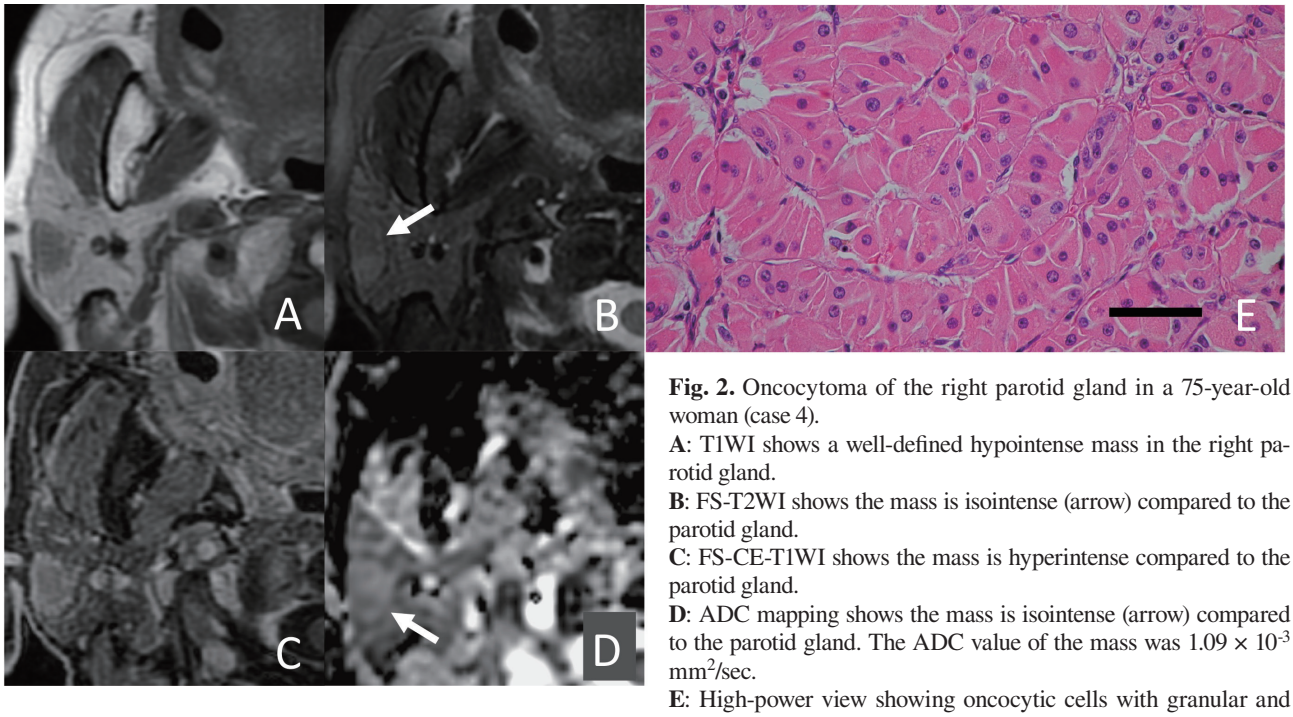

Fig. 2. Oncocytoma of the right parotid gland in a 75-year-old woman (case 4).
A: T1WI shows a well-defined hypointense mass in the right parotid gland.
B: FS-T2WI shows the mass is isointense (arrow) compared to the parotid gland.
C: FS-CE-T1WI shows the mass is hyperintense compared to the parotid gland.
D: ADC mapping shows the mass is isointense (arrow) compared to the parotid gland. The ADC value of the mass was 1.09×10^{-3} mm^2/sec.
E: High-power view showing oncocytic cells with granular and abundant cytoplasm and thin fibrovascular stroma (hematoxylin-eosin, scale bar = 25 μm).
ADC, apparent diffusion coefficient; FS-CE-T1WI, fat-suppressed postcontrast gadolinium-enhanced T1-weighted imaging; FS-T2WI, fat-suppressed T2-weighted imaging; T1WI, T1-weighted imaging.

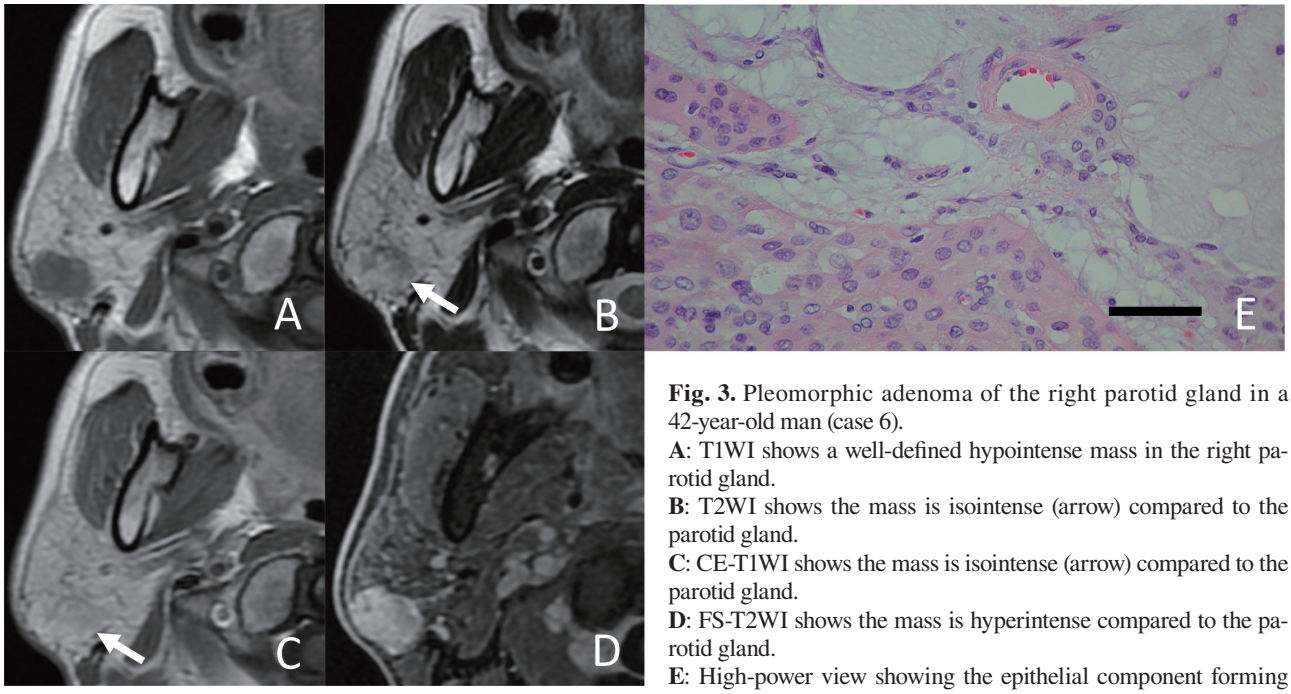

Fig. 3. Pleomorphic adenoma of the right parotid gland in a 42-year-old man (case 6).
A: T1WI shows a well-defined hypointense mass in the right parotid gland.
B: T2WI shows the mass is isointense (arrow) compared to the parotid gland.
C: CE-T1WI shows the mass is isointense (arrow) compared to the parotid gland.
D: FS-T2WI shows the mass is hyperintense compared to the parotid gland.
E: High-power view showing the epithelial component forming sheets (lower left) and a mesenchymal myxoid component (upper right) (hematoxylin-eosin, scale bar = 25 μm).
ADC, apparent diffusion coefficient; FS-CE-T1WI, fat-suppressed postcontrast gadolinium-enhanced T1-weighted imaging; FS-T2WI, fat-suppressed T2-weighted imaging; T1WI, T1-weighted imaging.

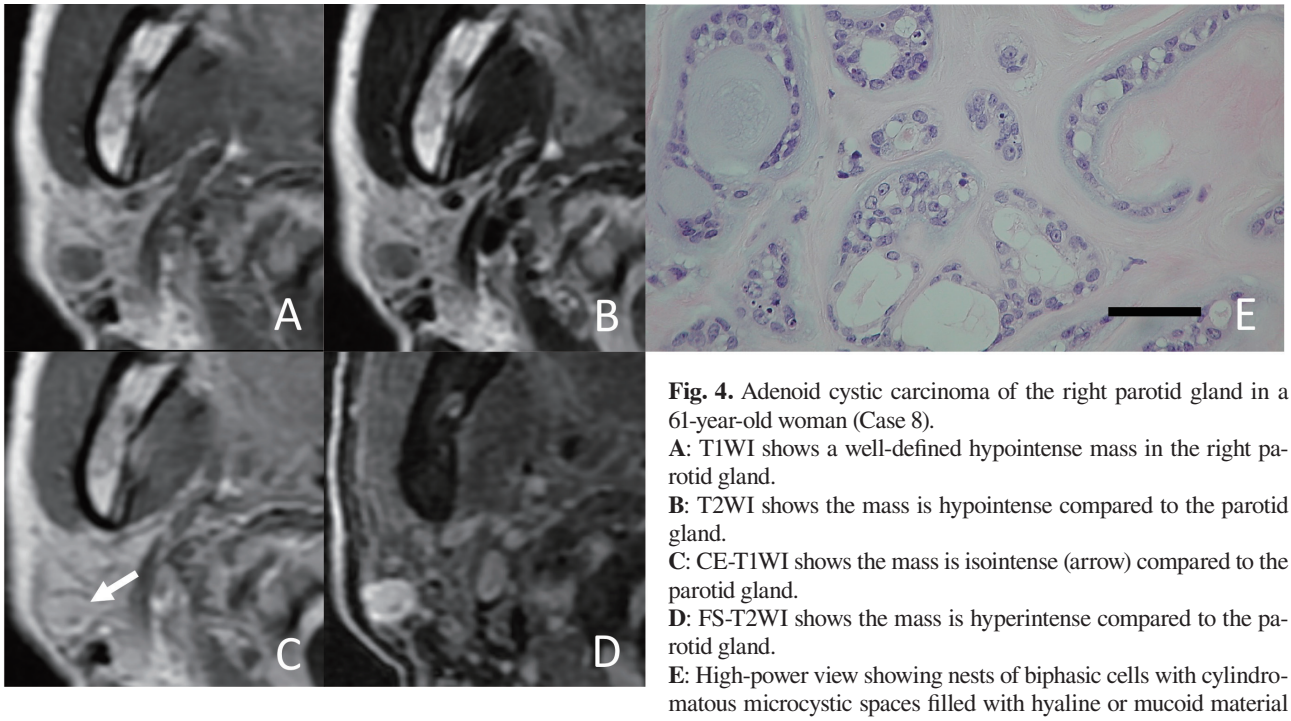

Fig. 4. Adenoid cystic carcinoma of the right parotid gland in a 61-year-old woman (Case 8).
A: T1WI shows a well-defined hypointense mass in the right parotid gland.
B: T2WI shows the mass is hypointense compared to the parotid gland.
C: CE-T1WI shows the mass is isointense (arrow) compared to the parotid gland.
D: FS-T2WI shows the mass is hyperintense compared to the parotid gland.
E: High-power view showing nests of biphasic cells with cylindromatous microcystic spaces filled with hyaline or mucoid material (hematoxylin-eosin, scale bar = 25 μm).
ADC, Apparent diffusion coefficient; FS-CE-T1WI, fat-suppressed postcontrast gadolinium-enhanced T1-weighted imaging; FS-T2WI, fat-suppressed T2-weighted imaging; T1WI, T1-weighted imaging.

3.4 cm^3 (range, 0.2–10.7 cm^3). The average diameter of all tumors was 1.7 cm (range, 0.7–2.5 cm). All tumors showed 'low' on T1WI and 'high' on DWI. Nine of ten tumors showed 'iso' on any other MR sequences. All Warthin tumors showed 'iso' on FS-T2WI, FS-CE-T1WI and ADC map (Fig. 1). One oncocytoma showed 'iso' on FS-T2WI and ADC mapping and 'high' on FS-CE-T1WI (Fig. 2). All pleomorphic adenomas showed 'iso' on T2WI and CE-T1WI (Fig. 3). One adenoid cystic carcinoma showed 'iso' only on CE-T1WI (Fig. 4), although one small cell carcinoma showed no 'iso' on any MR sequence.

DISCUSSION

It is generally accepted that the average size of parotid tumors at diagnosis is approximately 3 centimeters.[3] Patel et al. reported that eight of nine oncocytomas showed vanishing on both FS-T2WI and FS-CE-T1WI. The average cross-sectional diameter of the eight oncocytomas was 2.6 ± 0.7 cm (range, 1.3–3.3 cm).[2] This diameter is consistent with the average size of parotid tumors. In this study, the average diameter of all ten tumors showing homogeneous enhancement was 1.7 ± 0.7cm (range, 0.7–2.5 cm), smaller than that of typical parotid tumors. Furthermore, in addition to homogeneous enhancement, nine of the ten tumors showed vanishing. Hence, vanishing parotid tumors are likely among homogeneous tumors of small to average size.

In the present study, both Warthin tumors and oncocytoma showed hypointensity both on T2WI and CE-T1WI. Histologically, oncocytoma is composed of large epithelial cells with a characteristic bright eosinophilic granular cytoplasm, namely oncocytes. A thin fibrovascular stroma is also present.[4] Warthin tumors are composed of epithelial and lymphoid components. The epithelium comprises two layers of cells: large oncocytic cells and smaller basal cells. Lymphoid components with varying degrees of reactivity and with germinal centers are typical.[5] Therefore, both Warthin tumors and oncocytoma are hypercellular tumors with abundant microvessels. Generally, the cellular components are recognized as hypointensity on T2WI. In addition, hypointensity on conventional CE-T1WI is usually seen in hypercellular tumors showing early enhancement and a high washout rate on dynamic images. These findings are seen in benign tumors such as Warthin tumors and oncocytoma as well as in malignant tumors such as acinic cell carcinoma and malignant lymphoma.[6–9] In this study, both Warthin tumors and oncocytoma showed isointensity, namely vanishing, compared to the normal parotid glands on FS-T2WI. Furthermore, Warthin tumors showed vanishing, but oncocytoma showed hyperintensity on FS-CE-T1WI. Patel et al. reported that eight cases with oncocytoma showed vanishing both on FS-T2WI and FS-CE-T1WI.[2] The reason of the vanishing of oncocytoma in these MR sequences remains unclear. The hypointense tumor lesions on T2WI or CE-T1WI might show vanishing, namely, isointensity to normal parotid glands with decreased signal intensity due to fat signal suppression on FS-T2WI or FS-CE-T1WI. In the present study, both Warthin tumors and oncocytoma also showed vanishing on the ADC maps. This finding may be attributable to the high cellularity of these tumors, which show low ADC values nearly identical to those of the normal parotid gland. Interestingly, both oncocytoma and Warthin tumors show increased $^{99m}TcO^{4-}$ uptake on single photon emission computed tomography (SPECT) and also can exhibit increased fluorodeoxyglucose (FDG) uptake on positron emission tomography (PET).[10–12] Furthermore, Araki et al. reported that synchronous oncocytoma and Warthin tumor in the ipsilateral parotid gland had very similar imaging on CT, MRI, US and $^{99m}TcO^{4-}$ pertechnetate scintigraphy.[13] Hence, these tumors might have pathophysiological similarities as well as those histologic similarities.

In this study, pleomorphic adenomas showed vanishing both on T2WI and CE-T1WI, hyperintensity both on FS-T2WI and FS-CE-T1WI, and hyperintensity on ADC mapping. Pleomorphic adenoma is histologically composed of epithelial and myoepithelial cells and has mesenchymal elements. The epithelial component shows a wide variety of cell types, and the mesenchymal component is mucoid/myxoid, cartilaginous or hyalinised.[14] The T2-hyperintensity of pleomorphic adenomas, their increased ADC values, and their persistent enhancement after contrast administration are well-known as specific MRI findings consistent with fibromyxoid stroma.[15–17] Therefore, parotid tumors, including pleomorphic adenomas, that show T2-hyperintensity and persistent enhancement can show isointense to normal parotid gland and might also show vanishing on T2WI or CE-TIWI. Furthermore, the tumor lesions were considered to show hyperintensity compared to parotid glands with decreased signal intensity due to their fat signal suppression on FS-T2WI or FS-CE-T1WI.

Of the malignant tumors in the present study, only one adenoid cystic carcinoma with small size showed vanishing on CE-T1WI. Adenoid cystic carcinoma histologically consists of epithelial and myoepithelial cells and has stroma with hyalinized, mucinous or myxoid features.[18] The signal intensity of the adenoid cystic carcinoma might appear isointense to the parotid gland due to the tumor homogeneity associated with its small size and due to its persistent enhancement, which corre-

sponds to a rich interstitial space, similar to pleomorphic adenoma.[19]

In the present study, all tumors showed hypointensity on T1WI and hyperintensity on DWI, that is, they were depicted as conspicuous lesions on both T1WI and DWI. Meanwhile, vanishing of tumors was observed on T2WI, CE-T1WI, FS-T2WI, FS-CE-T1WI or ADC mapping. Therefore, isointense tumor lesions, compared to normal parotid glands, may be generally or partially overlooked on these sequences. Hence, MRI evaluation of parotid tumors should be performed initially by T1WI or DWI. Furthermore, considering the phenomenon of vanishing parotid tumors, careful evaluations of parotid glands on these sequences are necessary to avoid overlooking incidental parotid tumors.

Our study had several limitations. First, there was a problem with physiological fat depositions in parotid glands. Vanishing on MRI requires identical signals from parotid tumors and normal parotid glands. The extents of the physiological fat depositions of parotid glands varied in each case.[20] Accordingly, our qualitative evaluations of vanishing were influenced not only by parotid tumor characteristics but also by the variations of the fat depositions of the parotid gland. Second, we included limited types of parotid tumors. Vanishing of parotid tumors was observed in oncocytoma, Warthin's tumor, pleomorphic adenoma and adenoid cystic carcinoma in this study. Therefore, vanishing may occur in parotid tumors of other histological types. A larger study of patients with parotid tumors is required. However, this is the first report to evaluate vanishing of parotid tumors in various MR sequences.

In conclusion, vanishing of parotid tumors was observed in normal- to small-sized tumors on T2WI, CE-T1WI, FS-T2WI, FS-CE-T1WI and ADC mapping. No vanishing of tumors was observed on T1WI and DWI. Therefore, MRI evaluation of parotid tumors should be performed initially by T1WI or DWI. Furthermore, vanishing of tumors on FS-T2WI and FS-CE-T1WI, which is considered characteristic of oncocytoma, can be observed in Warthin tumors.

Acknowledgments: We are grateful for the expert assistance from the members of the Department of Radiological Technology, Tottori Prefectural Central Hospital.

The authors declare no conflict of interest.

REFERENCES

1 Kei PL, Tan TY. CT "invisible" lesion of the major salivary glands a diagnostic pitfall of contrast-enhanced CT. Clin Radiol. 2009;64:744-6. PMID: 19520223.
2 Patel ND, van Zante A, Eisele DW, Harnsberger HR, Glastonbury CM. Oncocytoma: the vanishing parotid mass. AJNR Am J Neuroradiol. 2011;32:1703-6. PMID: 21757520.
3 Cvetinović M, Stosić S, Jović N. How we have treated parotid gland tumors. Vojnosanit Pregl. 1997;54:45-52. PMID: 9354135.
4 Huvos AG. Oncocytoma. Barnes L, Eveson JW, Reichart P, Sidransky D, editors. World Health Organization Classification of Tumors: Pathology and Genetics, Head and Neck Tumors. Lyon: IARC Press; 2005. p. 266.
5 Simpson RHW, Eveson JW. Warthin tumour. Barnes L, Eveson JW, Reichart P, Sidransky D, editors. World Health Organization Classification of Tumors: Pathology and Genetics, Head and Neck Tumors. Lyon: IARC Press; 2005. p. 263-5.
6 Okahara M, Kiyosue H, Hori Y, Matsumoto A, Mori H, Yokoyama S. Parotid tumors: MR imaging with pathological correlation. Eur Radiol. 2003;13 Suppl 4:L25-33. PMID: 15018162.
7 Yabuuchi H, Fukuya T, Tajima T, Hachitanda Y, Tomita K, Koga M. Salivary gland tumors: diagnostic value of gadolinium-enhanced dynamic MR imaging with histopathologic correlation. Radiology. 2003;226:345-54. PMID: 12563124.
8 Ikeda M, Motoori K, Hanazawa T, Nagai Y, Yamamoto S, Ueda T, et al. Warthin tumor of the parotid gland: diagnostic value of MR imaging with histopathologic correlation. AJNR Am J Neuroradiol 2004;25:1256-62. PMID: 15313720.
9 Yabuuchi H, Matsuo Y, Kamitani T, Setoguchi T, Okafuji T, Soeda H, et al. Partotid gland tumors: can addition of diffusion-weighted MR imaging to dynamic contrast-enhanced MR imaging improve diagnostic accuracy in characterization? Radiology. 2008;249:909-16. PMID: 18941162.
10 Uchida Y, Minoshima S, Kawata T, Motoori K, Nakano K, Kazama T, et al. Diagnostic value of FDG PET and salivary gland scintigraphy for parotid tumors. Clin Nucl Med. 2005;30:170-6. PMID: 15722820.
11 Shah VN, Branstetter BF 4th. Oncocytoma of the parotid gland: a potential false-positive finding on 18F-FDG PET. AJR Am J Roentgenol. 2007;189:212-4. PMID: 17885033.
12 Sepúlveda I, Platín E, Spencer ML, Mucientes P, Frelinghuysen M, Ortega P, et al. Oncocytoma of the parotid gland: a case report and review of the literature. Case Rep Oncol. 2014;7:109-16. PMID: 24707257.
13 Araki Y, Sakaguchi R. Synchronous oncocytoma and Warthin's tumor in the ipsilateral parotid gland. Auris Nasus Larynx. 2004 Mar;31:73-8. PMID: 15041058.
14 Eveson JW, Kusafuka K, Stenman G, Nagao T. Pleomorphic adenoma. Barnes L, Eveson JW, Reichart P, Sidransky D, editors. World Health Organization Classification of Tumors: Pathology and Genetics, Head and Neck Tumors. Lyon: IARC Press; 2005. p. 254-8.
15 Tsushima Y, Matsumoto M, Endo K, Aihara T, Nakajima T. Characteristic bright signal of parotid pleomorphic adenomas on T2-weighted images with pathological correlation. Clin Radiol. 1994;49:485-9. PMID: 8088045.
16 Ikeda K, Katoh T, Ha-Kawa SK, wai H, Yamashita T, Tanaka Y. The usefulness of MR in establishing the diagnosis of parotid pleomorphic adenoma. AJNR Am J Neuroradiol. 1996;17:555-9. PMID: 8881252.
17 Motoori K, Yamamoto S, Ueda T, Nakano K, Muto T, Nagai Y, et al. Inter- and intratumoral variability in magnetic resonance imaging of pleomorphic adenoma: an attempt to interpret the variable magnetic resonance findings. J Comput Assist To-

mogr. 2004;28:233-46. PMID: 15091129.
18 EI-Naggar AK, Huvos AG. Adenoid cystic carcinoma. Barnes L, Eveson JW, Reichart P, Sidransky D, editors. World Health Organization Classification of Tumors: Pathology and Genetics, Head and Neck Tumors. Lyon: IARC Press; 2005. p. 221-2.
19 Tsushima Y, Matsumoto M, Endo K. Parotid and parapharyngeal tumours: tissue characterization with dynamic magnetic resonance imaging. Br J Radiol. 1994;67:342-5. PMID: 8173873.
20 Scott J, Flower EA, Burns J. A quantitative study of histological changes in the human parotid gland occurring with adult age. J Oral Pathol. 1987;16:505-10. PMID: 3127564.